THE JOURNAL OF BIOLOGICAL CHEMISTRY VOL. 280, NO. 42, pp. 35399–35409, October 21, 2005

Histidylated Lipid-modified Sendai Viral Envelopes Mediate Enhanced Membrane Fusion and Potentiate Targeted Gene Delivery*

Received for publication, June 17, 2005, and in revised form, July 26, 2005 Published, JBC Papers in Press, August 5, 2005, DOI 10.1074/jbc.M506615200

Santosh K. Verma[‡1,2], Prashant Mani[‡1], Nishi Raj Sharma[‡1], Anuja Krishnan[‡], Valluripalli Vinod Kumar[§], Bathula Surendar Reddy[§], Arabinda Chaudhuri[§], Rajendra P. Roy[¶], and Debi P. Sarkar[‡3]

From the [‡]Department of Biochemistry, University of Delhi South Campus, Benito Juarez Road, New Delhi 110021, the [§]Division of Lipid Science and Technology, Indian Institute of Chemical Technology, Uppal Road, Hyderabad 500007, and the [¶]National Institute of Immunology, Aruna Asaf Ali Marg, New Delhi 110067, India

Recent studies have demonstrated that covalent grafting of a single histidine residue into a twin-chain aliphatic hydrocarbon compound enhances its endosome-disrupting properties and thereby generates an excellent DNA transfection system. Significant increase in gene delivery efficiencies has thus been obtained by using endosome-disrupting multiple histidine functionalities in the molecular architecture of various cationic polymers. To take advantage of this unique feature, we have incorporated L-histidine (*N*,*N*-di-*n*-hexadecylamine) ethylamide (L_H) in the membrane of hepatocyte-specific Sendai virosomes containing only the fusion protein (F-virosomes (Process for Producing a Targeted Gene (Sarkar, D. P., Ramani, K., Bora, R. S., Kumar, M., and Tyagi, S. K. (November 4, 1997) U. S. Patent 5,683,866))). Such L_H-modified virosomal envelopes were four times more ($p < 0.001$) active in terms of fusion with its target cell membrane. On the other hand, the presence of L_H in reconstituted influenza and vesicular stomatitis virus envelopes failed to enhance spike glycoprotein-induced membrane fusion with host cell membrane. Circular dichroism and limited proteolysis experiments with F-virosomes indicated that the presence of L_H leads to conformational changes in the F protein. The molecular mechanism associated with the increased membrane fusion induced by L_H has been addressed in the light of fusion-competent conformational change in F protein. Such enhancement of fusion resulted in a highly efficient gene delivery system specific for liver cells in culture and in whole animals.

Completion and annotation of the human genome sequence has significantly enhanced the possibility of using designer DNA for gene therapy. Nonetheless, in spite of the first gene therapy trial 14 years ago, and numerous clinical trials thereafter, successful gene therapy remains elusive. The three main hurdles of widespread belief have been bolstered as (i) delivery, (ii) delivery, and (iii) delivery (1). It turns out that the most up-hill task toward ensuring clinical success of gene therapy is to design safe, efficacious and target-specific transfection vectors. Toward designing such gene carriers, significant progress has been made on gene transfection by novel non-glycerol-based histidylated cationic amphiphiles, presumably via the endosome-disrupting properties of the histidine functionalities (2). Histidine residues in amphipathic peptide antibiotics are also known to promote efficient DNA delivery into mammalian cells *in vitro* by favoring endosomal escape of the DNA molecules at low pH (3). Complexes of recombinant adenoviruses and cationic lipids/polymers have been tested for the enhancement of therapeutic index for the treatment of cystic fibrosis (4). The beneficial role of such complexes was clearly envisaged by the amplification of binding and entry of adenovirus particles into host cells. However, despite all these encouraging results, its failure in targeted gene transfer in whole animal and inherent cytopathic/cytotoxic side effects limit its applications in liver gene therapy (5). Because liver is an ideal organ for somatic gene delivery as well as the therapeutic target for hepatic diseases (6), we had developed a virus-based liver-specific delivery system (F-virosomes (FV))[4] (34) efficient in transferring foreign genes into human hepatoblastoma cells (HepG2) in culture and mouse/rat hepatocytes *in vivo*. F-virosomes exploit the membrane fusogenic property of Sendai virus F glycoprotein and the high affinity terminal β-galactose-containing ligands (present on F glycoproteins) for the asialoglycoprotein receptors on the hepatocyte surface (7). Upon tight binding to the asialoglycoprotein receptors, F-virosomes undergo fusion both at the level of plasma membrane and endosomal membrane followed by receptor-mediated endocytosis and deliver the entrapped molecules into the cytosol (8–10). We also observed that fusion efficiency of Sendai virus F protein is much reduced in the absence of its native attachment glycoprotein, hemagglutinin neuraminidase (HN) (7). To overcome such impediments, we tested the efficacy of histidine functionality in disrupting endosomes. Thus, we have incorporated L_H molecules in the F-virosomal membrane and systematically assessed its ability to enhance the binding and fusion with the target cells (cultured hepatocytes and mouse liver) as monitored by transgene expression. We report for the first time that histidine functionality of a cationic amphiphile specifically enhances F glycoprotein-induced membrane fusion and

* This work was supported in part by Department of Biotechnology Project BT/PR3026/PID/04/135/2002 from the Government of India and Panacea Biotec Ltd. New Delhi Project R&D/DO/03/023. The costs of publication of this article were defrayed in part by the payment of page charges. This article must therefore be hereby marked "*advertisement*" in accordance with 18 U.S.C. Section 1734 solely to indicate this fact.

[1] These authors contributed equally to this work.

[2] Supported by a research fellowship from Indian Council of Medical Research, Government of India.

[3] To whom correspondence should be addressed: Dept. of Biochemistry, University of Delhi South Campus, Benito Juarez Road, New Delhi 110021, India. Tel.: 91-11-24111967; Fax: 91-11-24110283 or 24115270; E-mail: dpsarkar59@rediffmail.com.

[4] The abbreviations used are: FV, F containing virosomes; DPBS, Dulbecco's phosphate-buffered saline; EGFP, enhanced green fluorescent protein; F, fusion factor; FV(H), heat-treated F containing virosomes; GV, vesicular stomatitis virus G-glycoprotein containing virosomes; HA, influenza hemagglutinin; HN, hemagglutinin neuraminidase; HNFV, HN and F containing virosomes; L_C, *N*,*N*-di-*n*-hexadecyl-*N*-2-aminoethylamine; L_CFV(H), heat-treated L_CFV; L_CFV, L_C containing FV; L_H, L-histidine (*N*,*N*-di-*n*-hexadecylamine) ethylamide; L_H/cholesterol, liposomes of L_H and cholesterol with a molar ratio 1:2; L_HFV(H), heat-treated L_HFV; L_HFV, L_H containing FV; L_HGV, L_H containing GV; L_HHAV, L_H containing hemagglutinin containing virosomes; NBD-PE, *N*-4-nitrobenzo-2-oxa-1,3-diazole phosphatidylethanolamine; RITC-lysozyme, rhodamine isothiocynate-labeled lysozyme; RT, reverse transcription; WGA, wheat germ agglutinin; PBS, phosphate-buffered saline; RBC, red blood cell; HR, heptad repeat; Tricine, *N*-[2-hydroxy-1,1-bis(hydroxymethyl)ethyl]glycine.

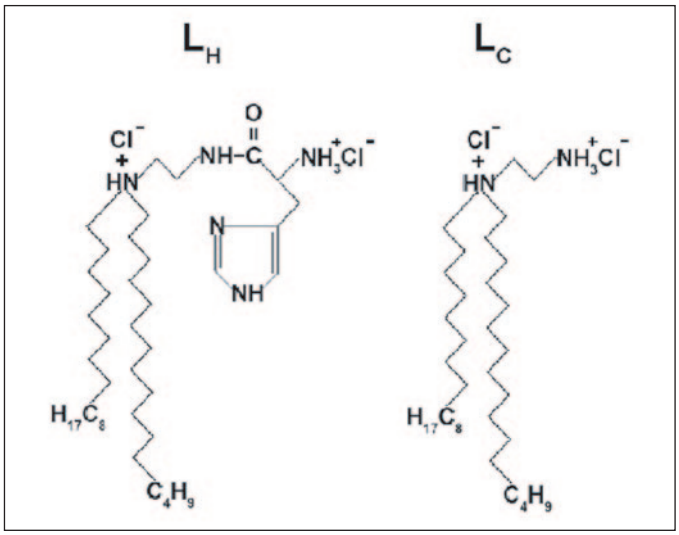

FIGURE 1. **Structure of lipids.**

results in efficient gene delivery.[5] The possible mechanisms of L_H-induced activation of F-virosome-target membrane fusion have also been investigated.

MATERIALS AND METHODS

Reagents

N-4-Nitrobenzo-2-oxa-1,3-diazole phosphatidylethanolamine (NBD-PE) was purchased from Avanti Polar Lipids. SM2 Bio-Beads were obtained from Bio-Rad. Triton X-100 was obtained from Aldrich. Lysozyme (chicken egg white, IUB 3.2.1.17), trypsin (type III), dithiothreitol, wheat germ agglutinin (WGA), sodium azide, EDTA (disodium salt), rhodamine isothiocyanate (RITC), bafilomycin A_1 were purchased from Sigma. L-Histidine (*N*,*N*-di-*n*-hexadecylamine) ethylamide (L_H) (molecular formula, $C_{40}H_{81}N_5C_{12}O$, molecular weight, 752.5) and *N*,*N*-di-*n*-hexadecyl-*N*-2-aminoethylamine (L_C) (molecular formula, $C_{34}H_{74}N_2C_{12}$, molecular weight, 581) were synthesized (Fig. 1) and stored as described earlier (2). Dulbecco's modified Eagle's medium, DPBS, fetal bovine serum, and antibiotics were obtained from Invitrogen. Monoclonal antibody against GFP was procured from BD Bioscience Clontech. VITROGEN® was purchased from COHESION Technologies Inc. (Palo Alto, CA). Other reagents used were also of the highest grade commercially available.

Virus

Sendai virus (Z strain) and influenza virus X:31 (A/Aichi/68;H3N2) were grown in the allantoic sac of 10–11-day-old embryonated chicken eggs. The virus was harvested and purified following standard procedures (7). Vesicular stomatitis virus (Indiana) was grown on monolayer cultures of baby hamster kidney (BHK-21) cells and purified as described elsewhere (11).

Cells

HepG2 cells (human hepatoblastoma cell line) and HeLa cells were obtained from American Type Culture Collection and were grown as described earlier (7). Fresh red blood cells were prepared from healthy Swiss albino mice in accordance with the norms of the Animal Ethics Committee, University of Delhi South Campus laws and regulations.

[5] Patent applied.

Preparation of Loaded F-virosomes

F-virosomes were prepared following published/patented procedures. Cationic amphiphiles (L_H and L_C) were incorporated in reconstituted viral membrane as described earlier for making NBD-PE-labeled virosomes (7). Briefly, the L_H and L_C compounds dissolved in solvents (chloroform:methanol, 2:1, v/v) were dried in a glass vial separately under nitrogen to form a thin film. The supernatant from the detergent extract of pure Sendai virus (50 mg of protein), containing only the viral F protein and the lipids, was added to the respective L_H and L_C films and incubated at 20 °C for 30 min with gentle shaking. The detergent was removed by SM2 Bio-Beads to form the virosomes. The amount of amphiphiles incorporated into the virosomal membranes (L_HFV and L_CFV) was analyzed by high performance liquid chromatography after purifying the virosomal preparations through a continuous sucrose gradient as described elsewhere (12). NBD-PE-labeled influenza virosomes (HA containing virosomes) with L_H and L_C were made according to earlier protocols with modifications as above (13). Similarly, labeled vesicular stomatitis virus virosomes (GV) with L_H and L_C were prepared following a published procedure (11). The plasmid pEGFP-N1 (Clontech, isolated using a Qiagen Megaprep unit) coding for enhanced green fluorescent protein (EGFP) under the control of cytomegalovirus promoter and RITC-lysozyme were entrapped in various virosomal preparations following our patented protocol (8, 10). Liposomes containing L_H/cholesterol and L_C/cholesterol were prepared as reported earlier (2). The virosome preparations were passed through 26-gauge needle 20 times and their particle size analyzed by a Photon Correlation Spectrometer (photon correlation spectrometry model: Photocor FC) using the software Flexcor/DynaLS provided by the Photocor company. The system was calibrated using 200-nm silica/latex particles (supplied by Photocor FC). Trypsinization, limited proteolysis by proteinase K, heat treatment (56 °C for 30 min), and DNase I digestion of virosome samples were carried as described elsewhere (8, 9, 14).

Membrane Fusion-mediated Targeted DNA/Protein Delivery to Cells in Culture

Hemolysis and lipid mixing (fluorescence dequenching of NBD-PE) assay for virosome-cell fusion were carried out as described earlier (7). Binding of NBD-PE-labeled virosomes and fusion-mediated delivery of RITC-lysozyme to the target cells were performed following our published protocol (7, 8). Targeted cytosolic delivery of pEGFP-N1 DNA to HepG2 cells in culture was essentially carried out as described elsewhere (9). For fusion-mediated delivery (of entrapped RITC-lysozyme and DNA) experiments to target cells in culture with bafilomycin A_1 (175 nM, a potent inhibitor of endosome acidification), the drug was mixed with loaded virosomes after dilution with the medium. The gene expression was assessed by recording EGFP fluorescence in a Nikon Eclipse TE 300 epifluorescent microscope attached to a digital camera (Digital sight DS-5M). For immunofluorescence studies, cells were washed with PBS twice and fixed in 2% paraformaldehyde in PBS at room temperature, followed by permeabilization with 0.1% Triton X-100 containing 0.5 M NH_4Cl in PBS for 10 min. The cells were blocked in 5% fetal bovine serum containing PBS at room temperature for 30 min and incubated with anti-GFP A.v. monoclonal antibody (JL-8) overnight at 4 °C followed by washing with PBS and incubation with fluorescein isothiocyanate-labeled goat anti-mouse IgG (Sigma). The cells were then visualized in a Nikon microscope for fluorescein isothiocyanate fluorescence as above. In a parallel assay, cell extracts were processed for evaluation of EGFP expression by Western analysis using the ECL detection system (Santa Cruz Biotechnology) and also by fluorometric quantitation (15). Total DNA/RNA isolation and PCR/RT-PCR amplification from the

cells in culture were performed as described below for *in vivo* studies with mice. All experiments were independently repeated at least three times.

Administration of Loaded Virosomes to Balb/c Mice and Gene Expression in Isolated Hepatocytes

Twelve-week-old female Balb/c mice (~18 g) were injected intravenously into the tail vein (in accordance with the guidelines of the Animal Ethics Committee, University of Delhi South Campus), with DNA-loaded virosomes (0.8 mg F protein containing 4 μg of pEGFP-N1) in a final volume of 0.2 ml of DPBS containing 2 mM Ca^{2+}. Injection of the equivalent amount of free DNA and heat-treated loaded virosomes in DPBS served as appropriate controls. After 2 days post-injection, parenchymal cell types (hepatocytes) were isolated as described in an earlier report by a member of our group (10) and plated on 12-well plastic plates (Falcon®, BD Biosciences) coated with VITROGEN® as per their protocol in Dulbecco's modified Eagle's medium with 10% fetal bovine serum. Following incubation in CO_2 for 24 h, plates were examined for EGFP expression as described above. The genomic DNA and total RNA were extracted by standard procedures (16) and subjected to PCR amplification/RT-PCR of the EGFP gene (transcripts).

(i) PCR Amplification of EGFP Gene—Total genomic DNA isolation from hepatocytes was done using TRIzol. The primer set designed for EGFP amplification included the following: sense, 5′-TGACCCT-GAAGTTCATCTGCACCA-3′; antisense, 5′-TTGATGCCGTTCT-TCTGCTTGTCG-3′. PCR amplification was performed using Taq DNA polymerase (Invitrogen) with a cycling profile of 94 °C for 45 s, 55 °C for 45 s, 72 °C for 45 s, for 30 cycles, and a final extension of 72 °C for 10 min (same in the case of β-actin primers, Stratagene). A specific amplified product of 361 bp of the EGFP gene was visualized by ethidium bromide staining on a 1.2% agarose gel and transferred to nylon membrane. As a control, the β-actin gene was also amplified and a product of 650 bp was obtained. Southern hybridization was performed to further confirm the specificity of the PCR products using a 720-bp NotI/HindIII EGFP gene fragment derived from the plasmid pEGFP-N1, labeled with [α-^{32}P]dCTP (by the random primer-labeling technique).

(ii) RT-PCR Amplification of EGFP Gene-specific Transcript—Total hepatic RNA from various mice or from HepG2 cells was isolated using TRIzol reagent (Invitrogen). DNase I (Invitrogen)-treated RNA was reverse transcribed using Superscript RNase H^- RT (Invitrogen) and gene-specific antisense primer as per the manufacturer's protocol. PCR amplification (30 cycles) of the RT product was performed using high-fidelity Platinum *Taq* DNA polymerase (Invitrogen) with a cycling profile as mentioned before. The amplified product of 361 bp of the EGFP gene was visualized by ethidium bromide staining on a 1.2% agarose gel and transferred to nylon membrane and subsequently Southern hybridized. As a control, β-actin mRNA was also amplified by RT-PCR for each sample and a product of 650 bp was obtained.

Luciferase Gene Expression in Parenchymal Liver Cells 48 h after Injection of pBVluc-loaded Virosomes to Balb/c Mice

Following intravenous (tail vein) injection (0.8 mg of F protein containing 4 μg of plasmid DNA) of various pBVluc (containing the firefly luciferase gene under control of the cytomegalovirus promoter as described earlier by Ramani *et al.* (10))-loaded virosomes (FV, L_CFV, L_HFV, and L_HFV(H)), parenchymal cells were isolated as above. The cells were washed twice with Tricine-buffered saline and suspended in the same. For luciferase assay, the Triton X-100-solubilized cell lysate (from 1×10^7 cells) was mixed with luciferase assay buffer containing 1 mM luciferin (Roche Molecular Biochemicals). Luciferase activity (in mV) was measured in a 1250 Luminometer (BIO-Orbit, Finland) as described earlier (10).

Histological and Immunohistochemical Methods

Four groups of mice (three mouse per group) were injected (0.8 mg of F protein containing 4 μg of plasmid DNA) with various pEGFP-N1-loaded virosomes (FV, L_CFV, L_HFV, and L_HFV(H)). After 6 months a portion of each liver from the injected mice was immediately fixed in Bouins fixative and dehydrated through graded alcohol and xylene followed by embedding in paraffin wax. Such embedded tissues were cut into 5-μm sections, deparaffinized, and rehydrated. For immunostaining, sections were washed in PBS for 10 min and blocked with 3% bovine serum albumin in PBS for 1 h at 37 °C. Subsequently, sections were incubated with EGFP-specific monoclonal antibody (JL-8) for 1 h at 37 °C. After three washes with PBS, sections were incubated with fluorescein isothiocyanate-labeled goat anti-mouse IgG at 37 °C for 1 h. All antibody dilutions were made in 1.5% bovine serum albumin in PBS. Following extensive washes with PBS, the slides were counterstained with Mayer hematoxylin, washed in distilled water, and mounted in glycerol. The specificity of immunostaining was verified by the use of PBS in place of primary antibody (data not shown). The sections were examined using fluorescence microscopy (Nikon fluorescein isothiocyanate filter set) and photographed (magnification, ×20).

Circular Dichroism

The CD spectra were recorded on a Jasco (J-715) spectropolarimeter fitted with a Peltier-based temperature controller (PTC-43). The instrument was calibrated with (+)-10-camphorsulfonic acid. Subsequently, the spectral measurements of the virosome samples (0.04 mg/ml F protein in L_HFV and L_CFV samples) were made using a 0.2-cm path-length cell at room temperature with constant purging of nitrogen. Each protein sample was subjected to 30 scans to obtain the final spectrum. The respective buffer baseline was subtracted from the spectra of the protein samples and data were presented as ellipticity expressed in millidegree.

RESULTS

Fusion of F-virosomes with Target Cell Membrane Is Enhanced by Histidylated Cationic Lipid—To evaluate the particle size, virosomal preparations were subjected to photon correlation spectrometry measurements. It revealed the mean diameter of FVs to be 181 nm, which conforms well to the average size reported earlier by transmission electron microscopy (17), on the other hand, L_HFV and L_CFV preparations were found to be 298 and 232 nm, respectively (data not shown). ξ potential measurements of these virosomes reflected net negative charge for FV and net positive charge for both L_HFV and L_CFV. The membrane fusion activity of F protein in FV is well correlated with its ability to hemolyse various RBCs upon WGA-mediated binding of F protein to cell surface sugar molecules (7). Therefore, to begin with mouse, RBC was chosen as appropriate target cells with a view to check and compare the efficiency of membrane fusion by various virosomal preparations in the presence of WGA. As shown in Fig. 2*a*, various doses of L_H molecules significantly enhanced the hemolytic activity of L_HFVs. With 2 mg, L_H incorporated into 50 mg of total Sendai virus protein resulted in a 4-fold increase in hemolytic activity. The specificity of the effect of L_H was established by parallel control with L_C (having the same amount of positively charged head group but lacks histidine moiety, Fig. 1), which did not affect hemolysis over FVs alone. Strikingly, same amount of L_H in L_H/CHOL liposomes mixed with FVs did not affect hemolysis over FVs alone. HNFVs, containing HN that markedly

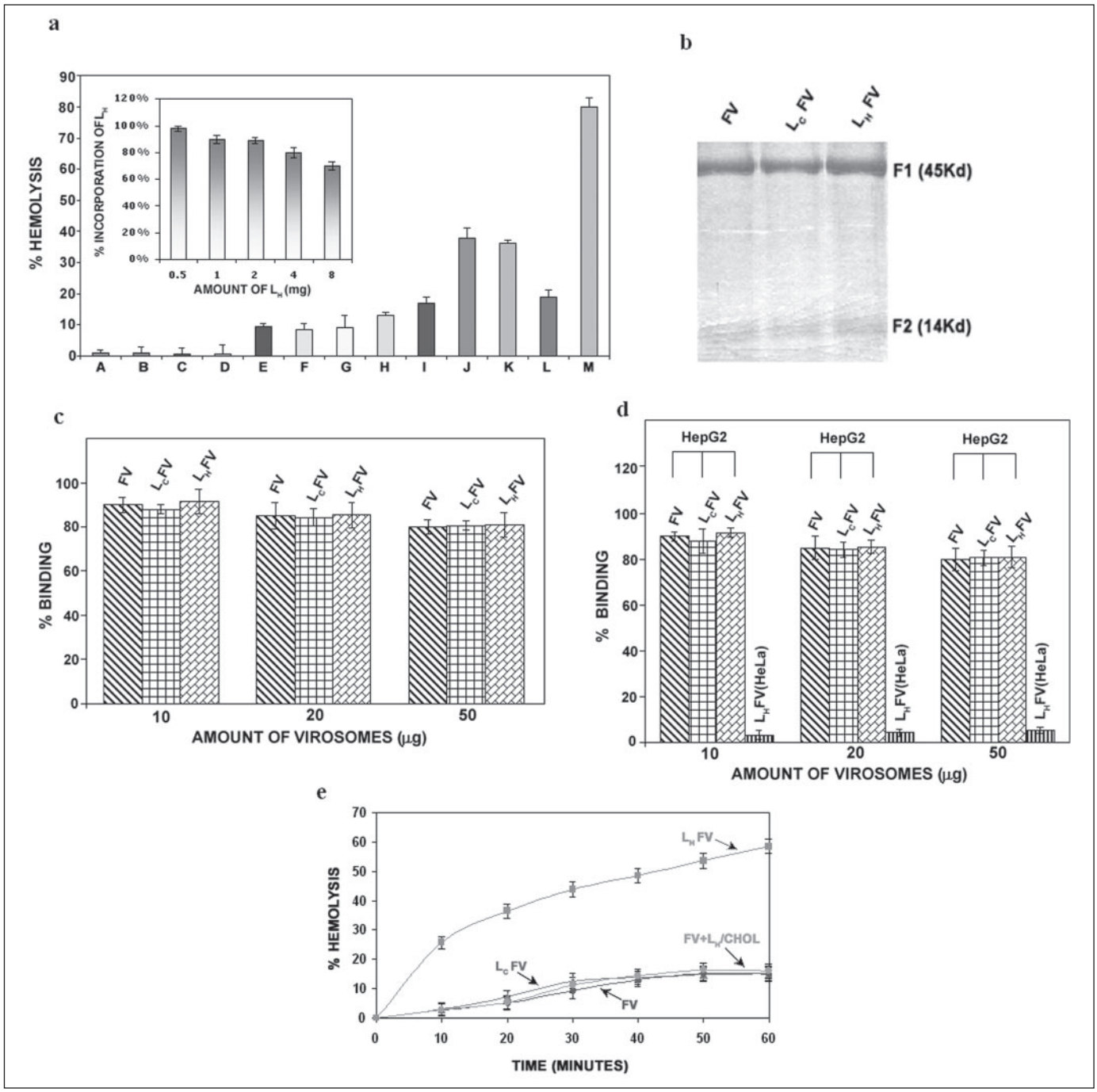

FIGURE 2. *a*, effect of L_H dose (and various treatments) on hemolysis of mouse RBCs induced by virosomes. Various virosomal preparations (20 μg of F protein) were added to mouse RBCs (0.5% v/v) in a total volume of 1 ml in PBS (pH 7.4), in the presence of 6 μg of WGA. The mixture was incubated on ice for 40 min with occasional shaking and then at 37 °C for 30 min. The reaction was terminated by chilling the mixture on ice and spun at 1,000 × *g* for 10 min. The amount of hemoglobin released in the presence of 0.3% Triton X-100 was taken as 100% lysis. The points are average of three independent experiments. *Inset* shows the dose-dependent incorporation of L_H in virosomal membrane. *A*, *FV*(*H*), heat-treated F containing virosomes; *B*, L_H*FV*(*H*), heat-treated L_HFV; *C*, L_C*FV*(*H*), heat-treated L_CFV; *D*, *T*.L_H*FV*, trypsin-treated L_HFV containing 2.0 mg of L_H; *E*, L_H/*CHOL*+*FV*, liposomes of L_H and cholesterol with a molar ratio 1:2 mixed with FV; *F*, L_C*FV*, L_C containing FV; *G*, FV, F containing virosomes; *H–L*, L_HFV containing 0.5, 1.0, 2.0, 4.0, and 8.0 mg of L_H, respectively; *M*, HNFV, HN, and F containing virosomes. *b*, electrophoretic mobility of various virosomes (20 μg of protein) resolved by SDS-10% PAGE and stained with Coomassie Blue. *c*, effect of L_H and L_C in binding of virosomes at 4 °C with mouse RBCs in the presence of 6 μg of WGA. NBD-PE-labeled virosomes were used to monitor binding in terms of fluorescence unit. The points are average of three independent experiments. *d*, effect of L_H and L_C in binding (in terms of NBD fluorescence measurement) of NBD-PE-labeled virosomes at 4 °C with HepG2/HeLa cells (in the presence of 10 mM sodium azide). As azide is known to completely inhibit endocytosis (8), the values reflect only the amount of virosomes bound to the surface of the cells. The points are average of three independent experiments. *e*, kinetics of hemolysis induced by virosomes. Virosomes (20 μg of protein) were added to mouse RBCs (0.5% v/v) in a total volume of 1 ml in PBS (pH 7.4), with 6 μg of WGA. The mixture was incubated at 4 °C for 60 min and then at 37 °C for different times. Hemolysis was measured (calculated as described in *a*) as a function of time. Each data point represents an average of three independent experiments.

enhances its lytic activity (7), served as a positive control, and incorporation of L_H and L_C molecules in HNFVs did not enhance the hemolytic activity any further. Similar results were also obtained with RBCs from human and rabbit (data not shown). The high performance liquid chromatography analysis of the sucrose density gradient-purified virosomes showed 85% efficiency of incorporation using 2 mg of L_H against 50 mg of Sendai virus (Fig. 2*a*, *inset*). The gradient purification of virosomes (12) ensured the co-grafting of L_H and L_C molecules with F protein in

the viral membrane. Similar profile of incorporation (and size) was also obtained with HA containing virosomes and GV (data not shown). The incorporation profile of L_C in FVs followed the same trend (data not shown). Calculations based on the protein/lipid composition of virosomes, molecular weights of F (HA and G) and cationic lipids, about 60 molecules L_H (and L_C), were estimated to be associated with one molecule of F (HA and G) protein in the respective virosomal membranes (having 2 mg of L_H with 50 mg of Sendai, influenza, and vesicular stomatitis virus). All further experiments were performed at this stoichiometry.

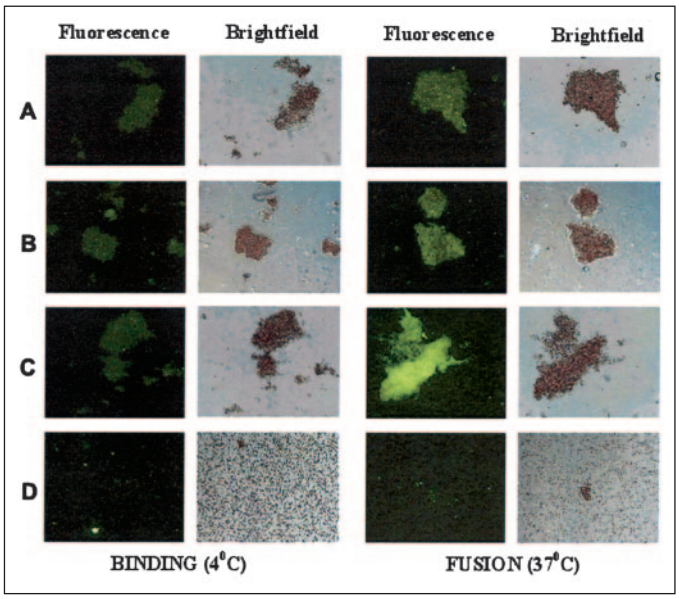

FIGURE 3. **Fusion of NBD-PE virosomes with mouse RBCs.** NBD-PE-labeled virosomes (10 μg of protein) were incubated at 4 °C for 60 min with 0.5% mouse RBCs in 1 ml of PBS (pH 7.4) containing 6 μg of WGA. The virosome-cell complexes were washed once at 300 × *g* (4 °C/2 min) in PBS, and cells were suspended in 1 ml of cold PBS. After 30 min incubation at 37 °C, cells were photographed with Nikon GFP filter set (magnification, ×10). *A*, FV; *B*, L_C FV; *C*, L_H FV; *D*, L_H FV(H). *H*, stands for heat-treated loaded virosomes.

NBD-PE-labeled FVs, L_HFVs, and L_CFVs, containing equivalent amounts of F protein of identical electrophoretic mobility (Fig. 2*b*), had equal affinity for mouse RBCs and HepG2 cells but showed negligible attachments to HeLa cells at 4 °C (Fig. 2, *c* and *d*). Because our main goal is to demonstrate targeted gene delivery in liver cells using L_H-modified FVs, HepG2 cells are included at this point as the only target cells of choice (7) to establish the role of L_H molecules in enhancing membrane fusion induced by F protein in culture conditions. HeLa cells are taken as negative controls to reveal the binding specificity of the terminal β-galactose moieties of F protein to the asialoglycoprotein receptors on the hepatocyte cell surface. As shown in Fig. 2*e*, the presence of L_H in the viral membrane markedly enhanced the kinetics (~8-fold increase) as well as the extent of hemolysis. L_H/cholesterol liposomes mixed with FVs failed to exert such an effect. Fluorescent micrographs showing escalated movement of NBD-PE (dequenching of fluorescence) from L_HFVs to mouse RBCs indicated membrane fusion (compare *panels A* and *B* with *C* in Fig. 3) and the transfer of RITC-lysozyme from loaded virosomes to an increased number (about 2-fold) of HepG2 cells (compare *panel 1* and *2* with *3* in Fig. 4*a*) indicated core mixing. This is also in agreement with higher (>3-fold) RITC fluorescence in HepG2 cells as in the case of L_HFV (Fig. 4*b*). It corroborated the fast kinetics (almost

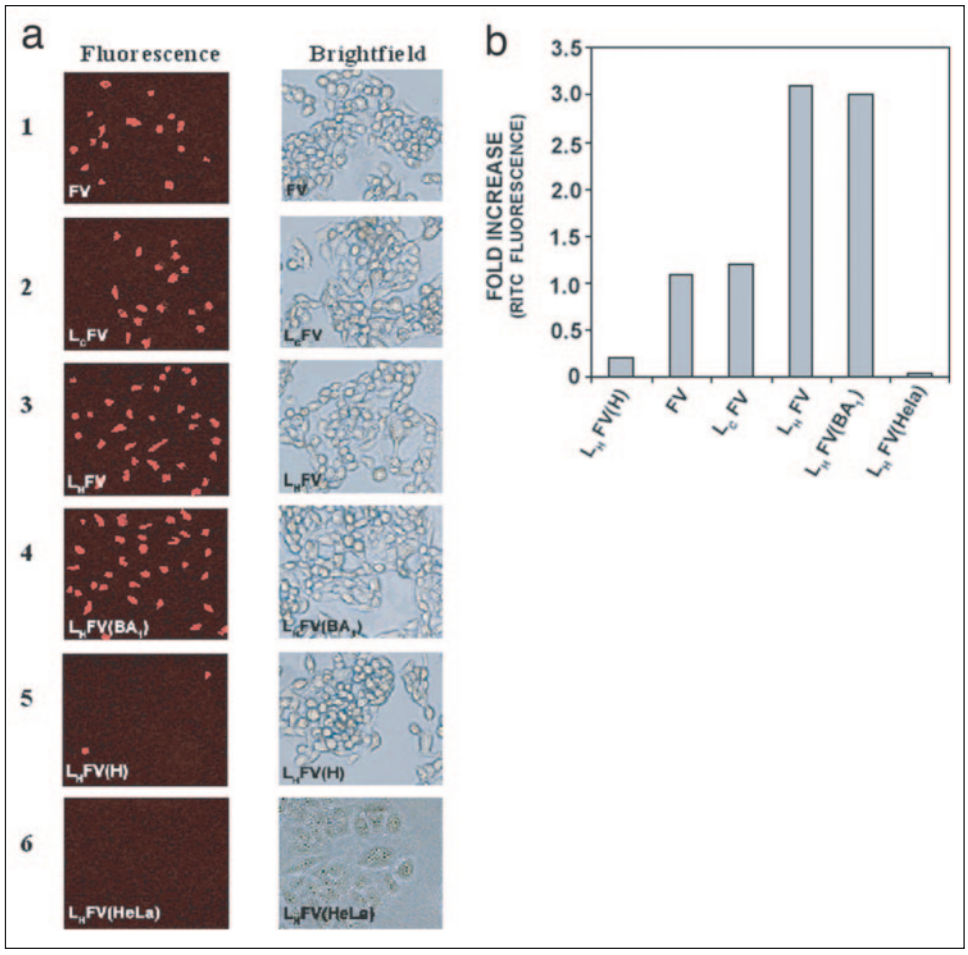

FIGURE 4. *a*, internalization of RITC-lysozyme into HepG2 cells delivered through virosomes. Loaded virosomes (40 μg of F protein, containing 4 μg of RITC-lysozyme) were incubated with HepG2 cells in 12-well culture plates. After incubation at 37 °C for 1 h, cells were washed with DPBS (pH 7.4) containing 5 mM EDTA (EDTA stripping to remove the bound but not fused virosomes with HepG2 cells as described by Bagai and Sarkar (8)) and subjected to fluorescence microscopy with a barrier filter of 590 nm (magnification, ×10). *1*, FV; *2*, L_CFV; *3*, L_HFV; *4*, L_HFV in presence of bafilomycin A_1; *5*, L_HFV(H); *6*, L_HFV incubated with HeLa cells. (*H*) stands for heat-treated loaded virosomes. *b*, -fold increase of RITC fluorescence (arbitrary units) in HepG2 cells. Upon fluorescence microscopy as in *a*, cell lysates were made following the procedure of Dandekar *et al.* (15) and fluorescence was measured in a spectrofluorometer taking an equal amount of proteins (100 μg). The values are average of three independent experiments.

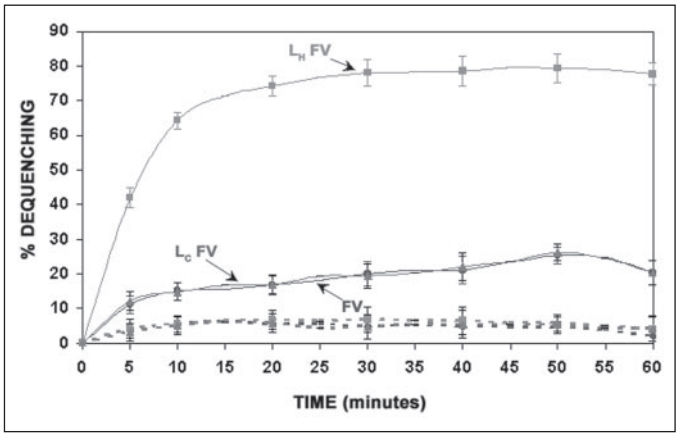

FIGURE 5. **Kinetics of membrane fusion (fluorescence dequenching (*FDQ*)) of NBD-PE-labeled various virosomes with HepG2 and HeLa cells.** Ten micrograms of NBD-PE-labeled virosomes were incubated at 4 °C for 40 min with 1×10^6 HepG2 or HeLa cells in 1 ml of DPBS (pH 7.4) containing 1.5 mM Ca^{2+}. Virosome-cell complexes were washed three times at 300 × *g* (4 °C/2 min) in cold DPBS buffer to remove unbound virosomes and cells were suspended in 1 ml of prewarmed DPBS and incubated at 37 °C for various times. Fluorescence was measured at 473/520 nm (excitation/emission) wavelengths with a spectrofluorometer (model RF-540, Shimadzu Corp, Kyoto, Japan). Percent fluorescence dequenching (%FDQ) was calculated according to the equation: $\%FDQ = 100 \times F - F_0/F_t - F_0$, where *F* and F_t are fluorescence units at a given time point and in the presence of 0.3% Triton X-100, respectively, and F_0 is fluorescence at time 0. Each data point represents an average of three independent experiments. *Solid lines*, HepG2 cells; *dotted lines*, HeLa cells.

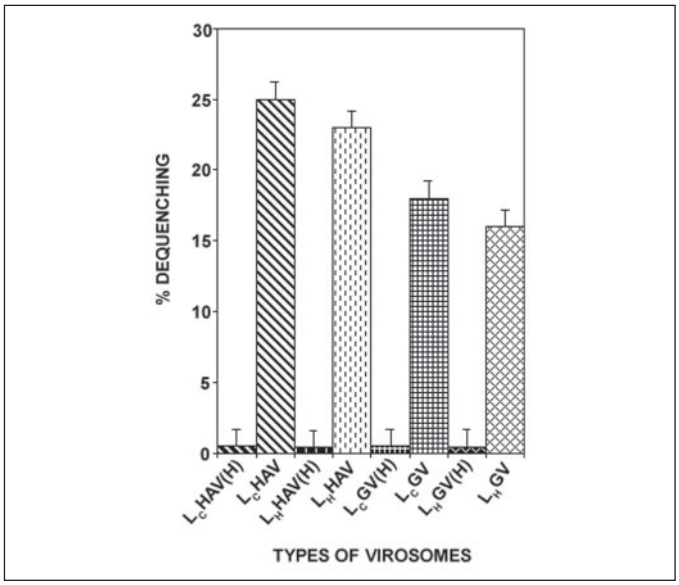

FIGURE 6. **Effect of L_H on fusion (fluorescence dequenching) of NBD-PE-labeled influenza HA (X31) and vesicular stomatitis virus G virosomes with HepG2 cells.** Ten micrograms of various NBD-PE virosomes were incubated with 1×10^6 HepG2 cells separately at 4 °C for 40 min in 1 ml of DPBS containing 1.5 mM Ca^{2+}. After removing unbound virosomes as in Fig. 5, the bound virosome-cell suspension was placed into a cuvette containing 1 ml of DPBS (pH 5.0), prewarmed to 37 °C, and fluorescence measurements were made after 30 min as described in the legend to Fig. 5. Values indicated are average of three independent experiments. *L_CHAV* and *L_HHAV* denote influenza HA (X31) containing virosomes with L_C and L_H, respectively. *L_CGV* and *L_HGV* denote vesicular stomatitis virus G containing virosomes with L_C and L_H, respectively. (*H*) denotes heat-treated virosomes.

4-fold) and higher extents of fluorescence dequenching of NBD-PE (Fig. 5) with target cells at neutral pH. Such accelerated movement of NBD-PE was not observed with FVs mixed with L_H/cholesterol liposomes (data not shown). It was also confirmed that at low temperature (4 °C), L_H in the virosomal membrane did not have any influence on binding to RBCs (Fig. 3, *panels A–C*) and HeLa cells (Fig. 2*d*). Hemolysis experiments carried out with DNA-loaded virosomes at pH 5.0 showed similar results (data not shown). Bafilomycin A_1, which inhibits endosome acidification by blocking the action of H^+-ATPase, could not diminish the fusion-mediated RITC-lysozyme transfer from L_HFVs (Fig. 4*a*, *panel 4*, during co-incubation, and also the 15 min pre- and postincubation condition results were the same as that of co-incubation, data not shown). L_H/cholesterol liposomes, when co-incubated with all types of loaded virosomes, did not affect at all the F protein-mediated membrane fusion (membrane and core mixing events) at both pH 7.4 and 5.0 (data not shown). Notably, L_H could not influence the activation of HA and G protein-induced fusion of viral envelopes with HepG2 cells (Fig. 6).

L_H Containing F-virosomes Augment Targeted Gene Transfer in Vitro—To assess the effect of DNA loading on the size of various virosomes, the preparations were checked by photon correlation spectrometry analysis. Upon entrapment of pEGFP-N1 DNA in FVs (50 μg of DNA/mg of F protein), the size of the loaded virosomes showed a slight increase to 232 nm, whereas, the same amount of DNA loaded in L_CFVs and L_HFVs (80 μg of DNA/mg of F protein) exhibited an almost 2-fold increase (data not shown). However, as observed with FVs earlier (9), all three types of FV-associated DNA was found to be DNase I resistant, indicating that it was entrapped rather than adsorbed on the virosomal membrane. No detectable leakage of DNA was observed from such loaded vesicles incubated with PBS or mouse plasma/fetal bovine serum at 37 °C for about 6 h and heat-treated virosomes (56 °C for 30 min). Membrane fusion activity of these loaded preparations was assessed by their ability to lyse mouse RBCs and fuse with HepG2 cells in culture and found to be very similar to that of their unloaded counterparts (data not shown).

With a view to evaluate the efficiency of gene expression mediated by L_HFVs, 4 μg of pEGFP-N1 DNA-loaded virosomes were incubated with HepG2 and HeLa cells for 24 h in the culture medium. More than 60% of the HepG2 cells expressed EGFP protein as shown in Fig. 7*a*, *panel 4*, under the influence of L_H lipid, whereas FV and L_CFVs showed around 20–30% EGFP positive cells (Fig. 7*a*, *panels 2* and *3*, respectively). Three to 4-fold enhancement of gene expression is also corroborated by quantitating fluorescence in the cell extracts (Fig. 7*b*). Heat-treated L_HFVs (Fig. 7*a*, *panel 1*) and L_HFVs incubated with HeLa cells (Fig. 7*a*, *panel 6*) failed to express EGFP. However, in the presence of bafilomycin A_1, transfection efficiency remained unchanged (Fig. 7*a*, *panel 5*) as observed in the case of lysozyme transfer (Fig. 4*a*). These results were further verified with immunofluorescence studies (data not shown) using specific anti-GFP antibody upon fixing the same cells as in Fig. 7*a*. To obtain further support of the expression profile of EGFP expression in various treatments, cells were processed for Western blot analysis (Fig. 7*c*, *panel A*) and a high level expression (about 3-fold more) was reconfirmed in the case of loaded L_HFVs. To determine whether the observed differences in gene expression were because of varying efficiencies of DNA delivery and differential transcript synthesis, DNA-PCR and RT-PCR were performed, followed by Southern analysis from cells in a parallel experiment (results presented in Fig. 7*c*, *panel B* and *C*, respectively). A careful comparison of the Southern hybridized specific band intensities with a standard curve (Fig. 7*c*, *panel D*), revealed ~2[1,2]-fold more delivery of EGFP DNA under L_H influence, keeping the number of HepG2 cells fixed. Thus, a direct correlation between the amount of delivered DNA and the level of transgene expression was observed.

Site-specific Gene Delivery in Whole Animal through L_HFV—To ensure that the transgene expression was exclusive for hepatocytes (in conformity with the cell-specific nature of the virosomal delivery system, in vivo), cells isolated from various organs of mouse, 2 days after injection of 4 μg of DNA-loaded virosomes, were analyzed for EGFP

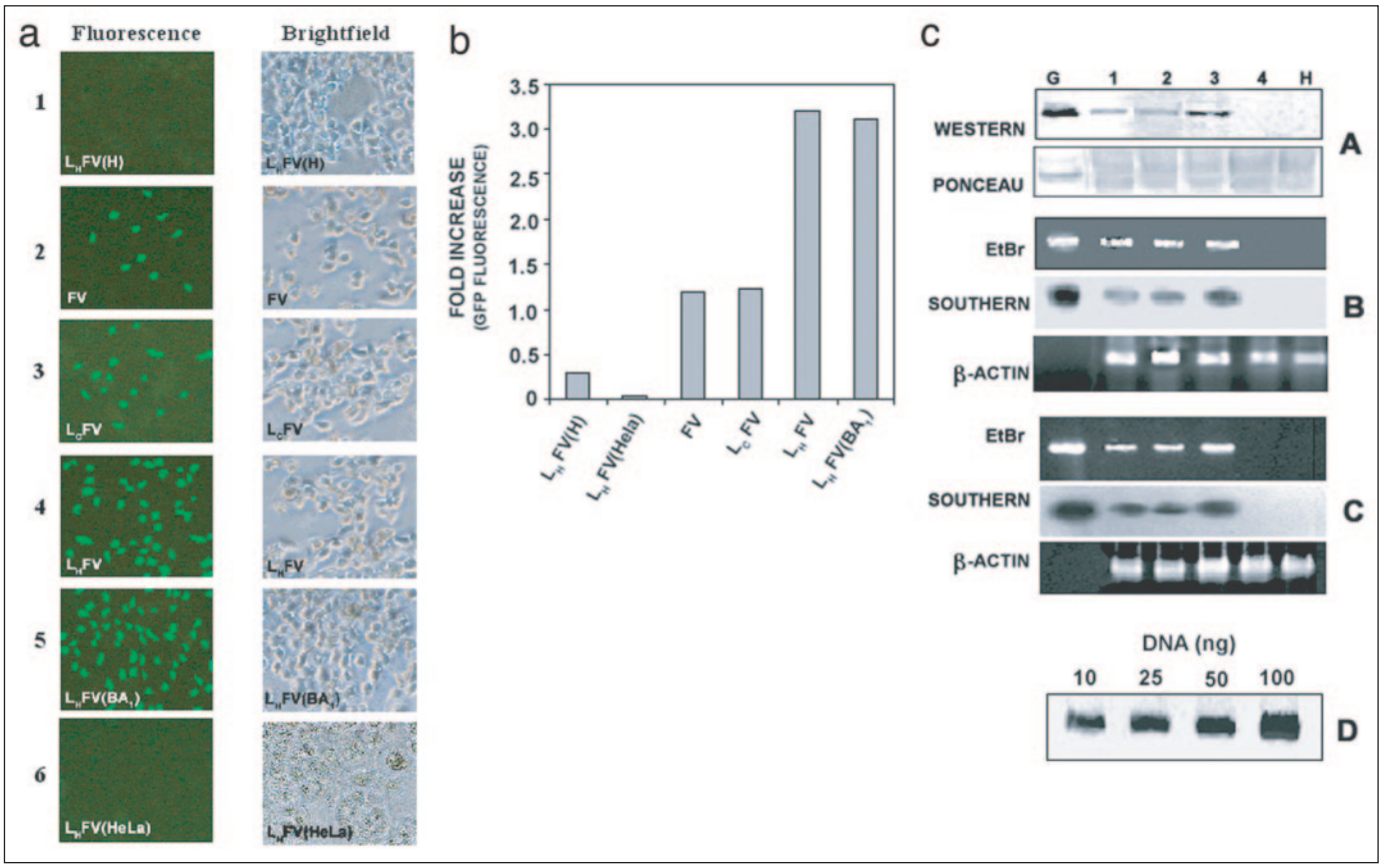

FIGURE 7. *a*, expression of EGFP in HepG2 cells transfected with DNA-loaded virosomes as described under "Materials and Methods." After incubation for 24 h, cells were subjected to fluorescence microscopy (Nikon eclipse TE 300, Japan) and photographed with a barrier filter of 510 nm (magnification, ×10). *1*, $L_HFV(H)$; *2*, FV; *3*, L_CFV; *4*, L_HFV; *5*, L_H FV in the presence of bafilomycin A_1; *6*, L_HFV incubated with HeLa cells. *b*, -fold increase of EGFP fluorescence (arbitrary units) in HepG2 cells. This was carried out as described in the legend to Fig. 4*b*. The points are average of three independent experiments. *c*, critical evaluation of EGFP expression. Western blot analysis of EGFP expressed in HepG2 cells in culture, using anti-GFP antibody. Corresponding Ponceau S-stained proteins on nitrocellulose membrane reflect loading control (*panel A*), DNA PCR (*panel B*), RT-PCR (amplification of EGFP mRNA using EGFP-specific primers followed by hybridization with EGFP gene probe) (*panel C*), and Southern hybridization of standard pEGFP-N1 plasmid (*panel D*). DNA/RNA loading controls are visualized by β-actin expression. *G*, GFP control; *1*, FV; *2*, L_CFV; *3*, L_HFV; *4*, $L_HFV(H)$; *H*, HeLa.

gene expression. This was critically assessed in intact liver parenchymal cells at the level of protein (Fig. 8, *a* and *b*, and *panel A* of *c*), DNA (Fig. 8*c*, *panel B*), and mRNA (Fig. 8*c*, *panel C*). A remarkable transfection efficiency (>70% of the hepatocytes) was achieved with histidylated virosomes (Fig. 8*a*, *panel 4*) in terms of EGFP-positive liver cells, whereas greater than 20% of cells exhibited EGFP fluorescence in the case of FVs (Fig. 8*a*, *panel 2*) and L_CFVs (Fig. 8*a*, *panel 3*). Heat-treated L_HFVs failed to show detectable gene expression as expected (Fig. 8*a*, *panel 1*). Similar -fold increase in EGFP expression (~3-fold) was substantiated from the fluorescence quantitation (Fig. 8*b*). This superior nature of histidyl induction of fusion-mediated cytosolic delivery, *in vivo*, was further corroborated with immunofluorescence analysis with the fixed cells (data not shown) and Western analysis (about 2.5-fold more over controls) in parallel experiments (Fig. 8*c*, *panel A*). DNA-PCR analysis of two mice (Fig. 8*c*, *panel B*) (and repeated three times) reflected almost 2-fold more delivery of DNA by loaded L_HFVs over FVs and L_CFVs to the hepatocytes. RT-PCR analysis of total RNA from isolated hepatocytes (Fig. 8*c*, *panel C*) matched higher DNA delivery. Failure of the detection of EGFP transcripts in other organs confirmed the liver-specific delivery of loaded-L_HFVs in whole animal (Fig. 8*c*, *panel D*). Moreover, total lymphocytes from blood and cells isolated from the organs other than liver did not exhibit any EGFP fluorescence (data not shown). Furthermore, luciferase gene expression profiles in isolated parenchymal cells (and no significant expression was found in non-parenchymal cells) from injected mice (Fig. 8*d*) and immunohistochemical analysis of EGFP expression in liver sections (Fig. 8*e*) reconfirmed the supremacy of L_HFV-mediated gene delivery and expression over FV, L_CFV, and other appropriate controls. Interestingly, expression of EGFP in whole liver was sustained until 6 months following a single injection of loaded virosomes and superior transfection efficiency (in terms of number of EGFP positive cells) of L_HFV over FV and L_CFV is further bolstered. The animals remained healthy and active during the experiments.

Histidylated Cationic Lipid Induces Conformational Changes in F Protein—Limited proteolysis experiments have been successfully used to probe changes in structure, dynamics, and function of proteins (18). We subjected FV, L_HFV, and L_CFV to proteinase K digestion to ascertain conformational changes in F protein because of the presence of the histidylated lipid, which might have enhanced the membrane fusogenic propensity of F protein. Because it is well known that membrane fusion induced by Sendai viral F protein with its target cells is pH independent and fuses both at the cell surface (neutral pH) and acidic endosomal milieu (12), proteolysis of F protein was carried out at pH 7.4 and 5.0. The SDS-PAGE analysis of the proteinase K digest shown in Fig. 9 (*a* and *b*) reveals that proteolysis of F protein occurs in much the same way at both pH values. However, F protein is significantly more susceptible to proteinase K digestion in the presence of histidylated lipid. Under identical conditions, about 80% of the protein is digested in L_HFV as compared with only 50% in FV and L_CFV. These results are indicative of a

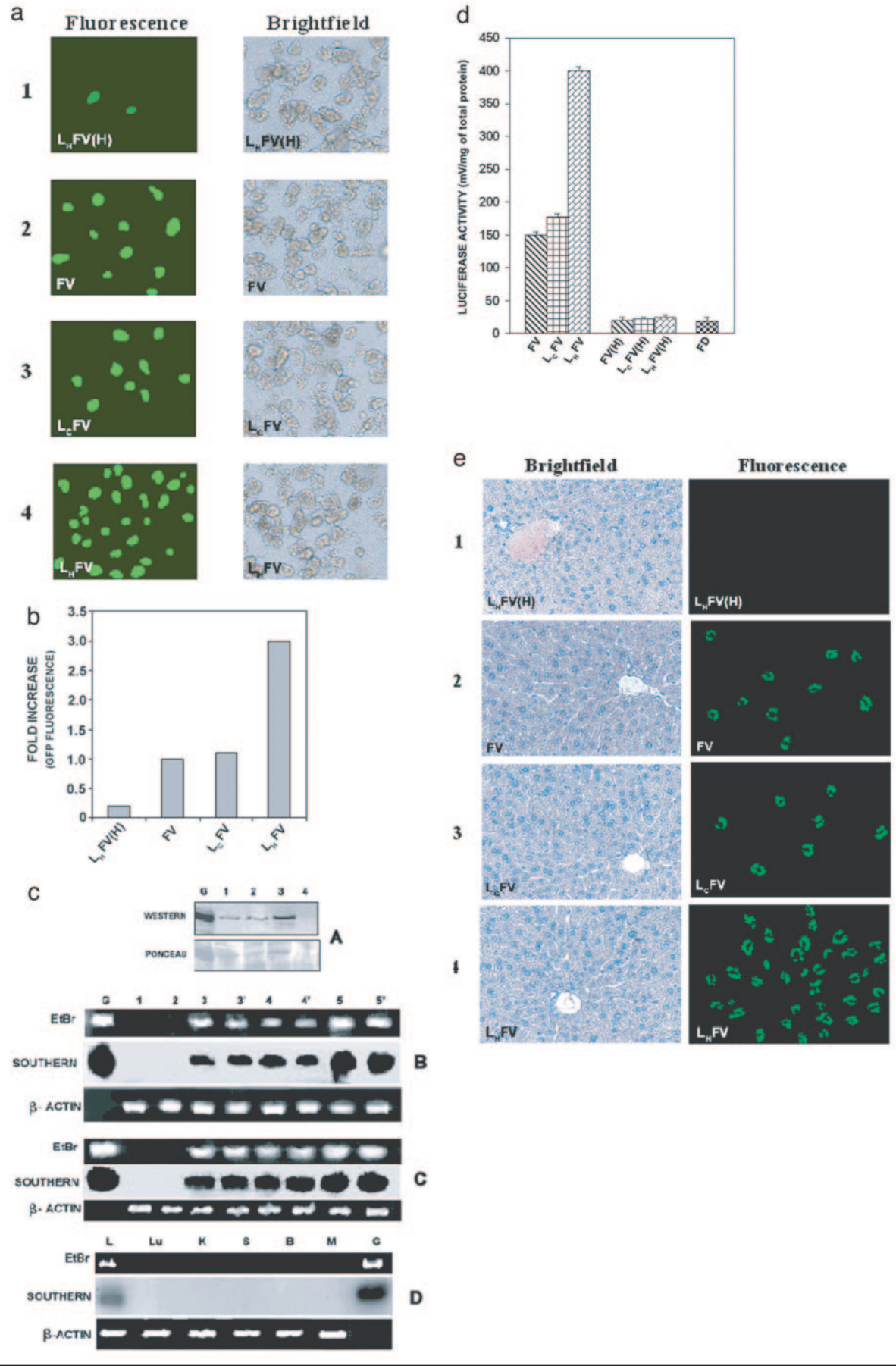

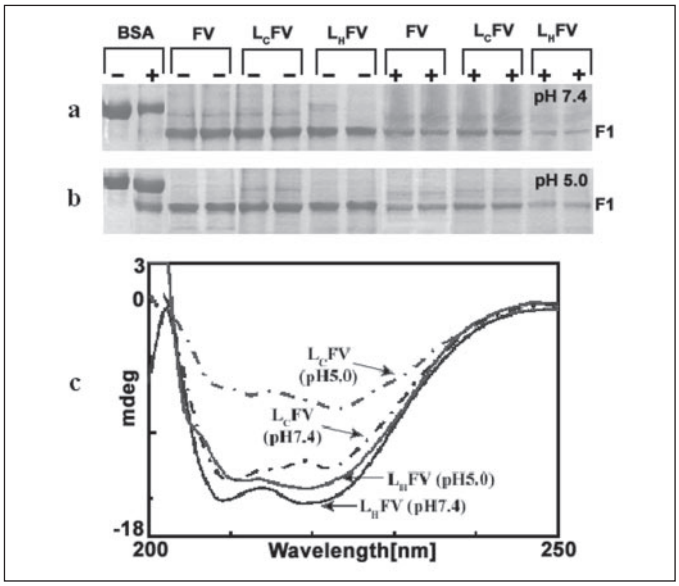

FIGURE 9. *a* and *b*, effect of L_H incorporation on the susceptibility of F protein (in virosomes) to proteolytic digestion by proteinase K. SDS-PAGE stained with Coomassie Blue are visualized following treatment with (+) and without (−) proteinase K. *a* and *b* indicate digestion at pH 7.4 and 5.0, respectively. The percentage degradation was calculated by densitometric scanning using "total lab image software" (Amersham Biosciences). Duplicate samples are loaded on gels. Bovine serum albumin (*BSA*) served as positive control. *c*, the CD spectra of L_HFV and L_CFV at pH 7.4 and 5.0 were recorded on a Jasco (J-715) spectropolarimeter as described under "Materials and Methods."

conformational change in F protein in the presence of the histidylated lipid.

Because L_HFV was relatively more susceptible to proteinase K digestion as compared with the L_CFV and FV, we examined the influence of histidylated lipid on the conformation of F protein by CD spectroscopy (Fig. 9*c*) at both pH 7.4 and 5.0 to mimic the plasma membrane and endosomal level fusion, respectively. For this, we recorded the far UV CD spectra of the F protein in the presence and absence of histidylated lipids. At both pH values (7.4 and 5.0), the spectra of the F protein exhibited double minima at 222 and 208 nm that are characteristics of the helical structure. The ellipticity value at 222 nm for F protein in the presence of L_HFV at pH 7.4 was about 15% higher than that of L_CFV. At pH 5.0, this difference was magnified to about 50% relative to L_CFV. Only a slight decrease in negative ellipticity at 222 nm was noticeable in L_HFV samples at pH 5.0 as compared with pH 7.4. In contrast, the negative ellipticity at 222 nm was considerably lower at pH 5.0 as compared with pH 7.4 in the case of L_CFV samples. L_H/cholesterol liposomes when mixed with FVs failed to induce any changes in the CD spectra. It is interesting to note that L_H molecules failed to induce any such structural alterations of HA and G proteins in their respective virosomes (data not shown). Taken together, the CD data indicate that the histidylated lipid exerts specific and significant influence on the secondary structure of F protein.

DISCUSSION

Sendai, an enveloped animal virus belonging to paramyxovirus family, contains two glycoproteins (hemagglutinin neuraminidase (HN) and fusion factor (F)) in the outer leaflet of its lipid bilayer (19). We have earlier established that besides conferring attachment function via sialic acid receptors, HN enhances F protein-mediated membrane fusion of reconstituted viral envelopes (F- and HN-virosomes) with target cells (7). Furthermore, loaded HN-depleted virus envelopes (F-virosomes) are known to selectively fuse with hepatocytes both in culture and in the whole animal leading to the delivery of proteins, drugs, DNA, and polymeric nanoparticles (10, 20–22). Considering a distinct role of HN in viral envelope-cell fusion and its lack of cell type specificity, it is felt that the F-virosome-mediated gene delivery system needs to be modified with suitable alternatives. Moreover, the molecular mechanism of HN-mediated help to F protein in terms of envelope-cell fusion (the fusion trigger) is yet to be deciphered (23). Working toward these two key objectives, we have presented evidence for significant enhancement of membrane fusion-mediated targeted cytosolic delivery of model drug and genes to liver cells by F-virosomes using a novel histidylated cationic amphiphile.

We first examined the hemolytic activity of the various virosome preparations (Fig. 2*a*) as it is closely related to its membrane fusion activity (7). This was then verified by more sensitive techniques, such as lipid and core mixing assays. Although a variation in size of various virosomes was noticed, the individual preparations were fairly homogeneous in size and emphasis was given to the same amount of protein taken in all cases (Fig. 2*b*). The reasons for size increase in the case of lipid-modified FVs are not yet clear. However, it is quite apparent that the lipids (L_H and L_C) did not influence the specific binding to mice RBCs (mediated through WGA, Fig. 2*c* and 3) and HepG2 cells (through F-asialoglycoprotein receptor interaction, Fig. 2*d*). Therefore, the possible role of L_H in activating the F protein could be ascribed to the histidyl moiety present in the same membranous milieu, at a stoichiometry of 60 molecules of L_H to one molecule of F protein. The failure of such enhancement of hemolysis by co-incubating L_H/cholesterol and FVs with RBCs supports this notion. Moreover, the fact that trypsinized L_HFVs could neither bind to RBCs (data not shown) nor cause any hemolysis (Fig. 2*a*) led us to conclude the participation of such L_H-activated F proteins in mediating such enhanced membrane fusion and that it is not because of any enhanced binding of virosomes to target cells through histidyl groups. Heat-treated L_HFVs (Fig. 2*a*) failed to induce hemolysis, thereby supporting the role of active F only in causing fusion with RBCs. Despite no remarkable reduction of incorporation of the L_H lipid in virosomal membranes (*inset* of Fig. 2*a*), the origin of the striking diminution of hemolysis above 4 mg of L_H cannot be explained presently. The fusion activation of F protein by L_H is bolstered by faster kinetics and a higher extent (about 8-fold) of hemolysis (Fig. 2*e*) and measurement of lipid mixing assay with RBCs through NBD-PE dequenching by fluorescence microscopy (Fig. 3, compare *panel C* with

FIGURE 8. *a*, *in vivo* expression of EGFP in mouse hepatocytes. Hepatocytes were isolated from mice, 48 h post-injection as described under "Materials and Methods." After 24 h incubation at 37 °C in a 5% CO_2 environment, cells were photographed for EGFP expression as described in the legend to Fig. 7*a* (magnification, ×20). *1*, L_HFV(H); *2*, FV; *3*, L_CFV; *4*, L_HFV. (*H*) stands for heat-treated loaded virosomes. *b*, -fold increase of GFP fluorescence (arbitrary units) in mouse hepatocytes. This was carried out as described in the legend to Fig. 4*b*. The points are average of three independent experiments. *c*, decisive assessment of EGFP expression. *Panel A*, Western blot of EGFP expressed in mouse hepatocytes using anti-GFP antibody and Ponceau S-stained proteins on nitrocellulose membrane (loading control); *G*, GFP control; *1*, FV; *2*, L_CFV; *3*, L_HFV; *4*, L_HFV(H). *Panel B*, DNA PCR. *Panel C*, RT-PCR of the total RNA isolated from the mouse hepatocytes; *G*, GFP control; *1*, L_CFV(H); *2*, L_HFV(H); *3*, FV; *3′*, FV; *4*, L_CFV; *4′*, L_CFV; *5*, L_HFV; *5′*, L_HFV. *Panel D*, RT-PCR amplification of EGFP mRNA from various organs of mice injected with DNA-loaded L_HFVs, using EGFP-specific primers followed by hybridization with EGFP probes; *L*, liver; *Lu*, lung; *K*, kidney; *S*, spleen; *B*, brain; *M*, skeletal muscle; *G*, GFP control. DNA/RNA loading controls are visualized by β-actin expression. *d*, luciferase gene expression in mouse hepatocytes mediated through histidylated lipid-modified virosomes. Luciferase activity in parenchymal cell types was determined as described under "Materials and Methods." Values represent mean (± S.D.) from three mice livers. *FD*, free DNA. *e*, efficient and persistent EGFP gene expression in whole mouse liver 6 months after injection of DNA-loaded virosomes. Immunohistochemical detection of the EGFP was carried out as described under "Materials and Methods" (magnification, ×20). *1*, L_HFV(H); *2*, FV; *3*, L_CFV; *4*, L_HFV. (*H*) stands for heat-treated loaded virosomes.

A and *B* under "Binding and Fusion"). It is well established that the fluorescence emission of NBD-PE remains quenched in the virosomal membrane because of its high-density packing. Upon fusion of the virosomal membrane with the target membrane, the phenomenon of "lipid mixing" ensures the transfer of NBD-PE molecules to the target cell membranes with concomitant dequenching of its fluorescence (7). The effect of L_H on the core mixing assay by transfer of RITC-lysozyme from L_HFVs to HepG2 cells in culture (Fig. 4, *a*, compare *panel 3* with *1*, and *2* and *b*) further confirms the enhanced and target-specific fusion-mediated delivery of virosomal contents at physiological pH. Similar results were obtained at pH 5.0 (data not shown) conforming the well established pH-independent fusion activity of Sendai virus (23). In an attempt to assess the proposed endosome disrupting nature of L_H (2) at pH 5.0 and its role if any, on the observed high efficiency of fusion of L_HFVs, a specific and potent proton pump inhibitor, bafilomycin A_1, completely failed to affect the fusion-mediated delivery of RITC-lysozyme (Fig. 4*a*, *panel 4*). Similarly, histidine-rich amphipathic peptide-mediated promotion of efficient DNA delivery into mammalian cells in culture was not found to be fully bafilomycin A_1-sensitive, indicating that protonation of histidine is not solely responsible for endosome disruption (3). The more pronounced effect (>6-fold) of L_H on kinetics of fusion of NBD-PE-labeled L_HFVs with HepG2 cells emphasizes the influence of the histidyl moiety in enhancing F-induced membrane fusion at both early and late events (Fig. 5). Furthermore, failure of L_H in affecting the membrane fusion of other analogous envelope spike glycoproteins (HA and G) indicates the specificity of L_H-F interplay (Fig. 6). Taken together, these results are in support of the belief that histidine head group-F protein cross-talking, analogous to HN-F interactions, is the key event in achieving such quantum jump in fusion activity.

About 2-fold increase in the diameter of lipid-modified DNA-loaded virosomes (L_CFVs and L_HFVs) is consistent with that of the liposomes formed with L_H and DNA (2). However, the maximum size with a mean diameter 532 nm of DNA-loaded L_HFVs did not exhibit any deviation of fusion function from their unloaded counterparts (data not shown) and could selectively deliver DNA to the HepG2 cells in culture (Fig. 7) and hepatocytes in mouse liver (Fig. 8). A remarkable increase in the targeted gene delivery and expression (>70% EGFP positive cells), aided by L_H in the case of L_HFVs both *in vitro* and *in vivo*, represents a significant development toward the goal of offering an entirely new and promising class of semiviral delivery vehicles. Furthermore, about 3-fold higher luciferase gene expression mediated through L_HFV (over FV and L_CFV) in mouse hepatocytes strengthens the role of L_H in achieving efficient gene transfer process (Fig. 8*d*). Additionally, the real beauty of L_HFV-mediated gene transfer is comprehended from the long lasting (6 months) and efficient EGFP expression in whole liver (Fig. 8*e*). It is relevant to state in this context, the safe and non-toxic issues of Sendai virus components in humans, extrapolating the studies with nonhuman primates (24). Some recent reviews and research articles on the area of gene delivery/therapy have underscored the importance of non-viral and liposomal/virosomal vectors in achieving successful gene therapy in the near future (25–28). Current clinical trials based on adenoviral vector-mediated gene transfer for curing inherited metabolic disorders have suffered serious setbacks following the death of Jesse Gelsinger in 1999 (26), and several other problems including toxic/immunogenic side effects, failure to integrate into host chromosomes, and low levels of transgene expression in human hepatocytes (non-replicating cells) (28). Despite removal of the viral genes in such vectors, potential safety concerns demand efficient non-viral methods for long-term gene transfer (25). Although several attempts have been made in the recent past, a high-pressure DNA delivery system ("hydrodynamic" methods) requires a very large volume of intravenous naked DNA injection into portal veins without any tissue/cell-specific targeting concerns (28). Moreover, safety issues are equally important and need to be sorted out. The present virosomal delivery system being truly at the interface of viral and non-viral vectors is expected to be adequately safe in comparison to their non-hybrid counterparts. Perhaps, with more similar manipulations, such modified virosomes will become increasingly difficult to discriminate from viruses and will suit the "liver gene therapy" protocol in reality.

Sendai virions exhibiting binding and fusion functions with host cells, contain the F protein in the form of a disulfide-linked complex ($F_{1,2}$), consisting of two glycopeptides (F_1 and F_2) that are derived by proteolytic cleavage of an inactive precursor (F_0) by a host cell enzyme (29). The movement of the fusion sequence to the target membrane prior to the culmination of fusion is believed to be facilitated by the formation of coiled-coil or helix bundle assembly of the N- and C-terminal heptad repeat (HR) sequences (30). Therefore, the stability of the secondary structure of this region is important in determining the rate and extent of fusion (31). Earlier studies (12) using reconstituted liposomes clearly indicate a significant increase in α-helicity during the cleavage of F_0 to $F_{1,2}$, reflecting the fusion competent conformation of F protein (F*). In the present study, CD analyses revealed increases in the helical conformation in F protein (in F-virosomes) in association with L_H at both neutral and acidic pH (Fig. 9*c*). However, the limited proteolysis experiments suggested that the F protein was more susceptible to proteolysis in the presence of histidylated lipid (Fig. 9, *a* and *b*). These results indicate that histidylated lipid might have stabilized the coiled-coil formation while partially unfolding the remainder of the molecule that became more sensitive to proteolysis. Taken together, the proteolysis and CD results in-frame with the fusion data support the notion of a gamut of conformational changes of F protein in association with L_H molecules. Induction of conformational changes of F protein by L_H may thus be presumed as the "super fusion-competent" (F**) form of F*. In this event, L_H help to the F*, may be conceptualized as a stabilizer of helicity of exposed hydrophobic HR sequence. The HR sequences are highly conserved among all paramyxovirus members and fold into a 6-fold helix bundle during the fusion process (23). The proposition of the F** state is in agreement with a recent study, where salient three-dimensional structural features of the fusion-primed Sendai F protein (F*) have been revealed by electron cryomicroscopy. It has been concluded that to expose the fusion peptide, the fusion-primed ectodomain of F* has to undergo further conformational changes (32). Additionally, an indirect support to our hypothesis on F* to F** transition, induced by L_H, may be drawn from a recent observation where a proline replacement of leucine at residue 705 in the heptad repeat region (HR2) of mitofusin reduces the stability of the HR2 coiled-coil with a concomitant reduction of mitochondrial membrane fusion (33). In the light of the well known HN-F interactions in the intact virions and its reconstituted envelopes containing both F and HN proteins (7), work is underway to test the exact contribution(s) of the histidine moiety to F protein in enhancing the fusion function. Notwithstanding the mechanism, the results presented here highlight the potential immediate applications of histidylated amphiphile-modified F-virosomes in liver "gene therapy."

Acknowledgments—We thank J. Roy-Chowdhury, S. Ghosh, A. Herrmann, H. P. Ghosh, S. K. Goswami, S. Dhar, S. Saxena, and R. Arora for stimulating discussions and constructive criticism.

REFERENCES

1. Luo, D. (2004) *Trends Biotechnol.* **22,** 101–103
2. Kumar, V. V., Pichon, C., Refregiers, M., Guerin, B., Midoux, P., and Chaudhuri, A. (2003) *Gene Ther.* **10,** 1206–1215
3. Kichler, A., Leborgne, C., März, J., Danos, O., and Bechinger, B. (2003) *Proc. Natl. Acad. Sci. U. S. A.* **100,** 1564–1568
4. Fasbender, A., Zabner, J., Chillón, M., Moninger, T. O., Puga, A. P., Davidson, B. L., and Welsh, M. J. (1997) *J. Biol. Chem.* **272,** 6479–6489
5. Cavazzana-Calvo, M., Thrasher, A., and Mavilio, F. (2004) *Nature* **427,** 779–781
6. Yamada, T., Iwasaki, Y., Tada, H., Iwabuki, H., Chuah, M. K., VandenDriessche, T., Fukuda, H., Kondo, A., Ueda, M., Seno, M., Tanizawa, K., and Kuroda, S. (2003) *Nat. Biotechnol.* **21,** 885–890
7. Bagai, S., Puri, A., Blumenthal, R., and Sarkar, D. P. (1993) *J. Virol.* **67,** 3312–3318
8. Bagai, S., and Sarkar, D. P. (1994)) *J. Biol. Chem.* **269,** 1966–1972
9. Ramani, K., Bora, R. S., Kumar, M., Tyagi, S. K., and Sarkar, D. P. (1997) *FEBS Lett.* **404,** 164–168
10. Ramani, K., Hassan, Q., Venkaiah, B., Hasnain, S. E., and Sarkar, D. P. (1998) *Proc. Natl. Acad. Sci. U. S. A.* **95,** 11886–11890
11. Paternostre, M.-T., Lowy, R. J., and Blumenthal, R. (1989) *FEBS Lett.* **243,** 251–258
12. Hsu, M., Scheid, A., and Choppin, P. W. (1981) *J. Biol. Chem.* **256,** 3557–3563
13. Bagai, S., and Sarkar, D. P. (1994) *FEBS Lett.* **353,** 332–336
14. Kumar, M., Hassan, M. Q., Tyagi, S. K., and Sarkar, D. P. (1997) *J. Virol.* **71,** 6398–6406
15. Dandekar, D. H., Kumar, M., Ladha, J. S., Ganesh, K. N., and Mitra, D. (2005) *Anal. Biochem.* **342,** 341–344
16. Sambrook, J., Fritsch, E. F., and Maniatis, T. (1989) *Molecular Cloning: A Laboratory Manual*, 2nd Ed., Cold Spring Harbor Laboratory Press, Cold Spring Harbor, NY
17. Bagai, S., and Sarkar, D. P. (1993) *Biochim. Biophys. Acta* **1152,** 15–25
18. Fontana, A., de Laureto, P. P., Spolaore, B., Frare, E., Picotti, P., and Zambonin, M. (2004) *Acta Biochim. Pol.* **51,** 299–321
19. Okada, Y. (1988) *Curr. Top. Membr. Transp.* **32,** 297–336
20. Bagai, S., and Sarkar, D. P. (1993) *FEBS Lett.* **326,** 183–188
21. Nijhara, R., Jana, S. S., Goswami, S. K., Rana, A., Majumdar, S. S., Kumar, V., and Sarkar, D. P. (2001) *J. Virol.* **75,** 10348–10358
22. Jana, S. S., Bharali, D. J., Mani, P., Maitra, A., Gupta, C. M., and Sarkar, D. P. (2002) *FEBS Lett.* **515,** 184–188
23. Lamb, R. A., and Kolakofsky, D. (2001) *Fields Virology*, 4th Ed., Lippincott, Williams and Wilkins, Philadelphia, PA
24. Tsuboniwa, N., Morishita, R., Hirano, T., Fujimoto, J., Furukawa, S., Kikumori, M., Okuyama, A., and Kaneda, Y. (2001) *Hum. Gene Ther.* **12,** 469–487
25. Niidome, T., and Huang, L. (2002) *Gene Ther.* **9,** 1647–1652
26. Branca, M. A. (2005) *Nat. Biotechol.* **23,** 519–521
27. Torchilin, V. P. (2005) *Nat. Rev. Drug Disc.* **4,** 145–160
28. Kren, B. T., Ghosh, S. S., Linehan, C. L., Roy-Chowdhury, N., Hackett, P. B., Roy-Chowdhury, J., and Steer, C. J. (2003) *Gene Ther. Mol. Biol.* **7,** 229–238
29. Scheid, A., and Choppin, P. W. (1977) *Virology* **80,** 54–60
30. Zhao, X., Singh, M., Malashkevich, V. N., and Kim, P. S. (2000) *Proc. Natl. Acad. Sci. U. S. A.* **97,** 14172–14177
31. Chen, Y. H., Yang, J. T., and Chau, K. H. (1974) *Biochemistry* **13,** 3350–3359
32. Ludwig, K., Baljinnyam, B., Herrmann, A., and Böttcher, C. (2003) *EMBO J.* **22,** 3761–3771
33. Koshiba, T., Detmer, S. A., Kaiser, J. T., Chen, H., McCaffery, J. M., and Chan, D. C. (2004) *Science* **305,** 858–862
34. Sarkar, D. P., Ramani, K., Bora, R. S., Kumar, M., and Tyagi, S. K. (November 4, 1997) U. S. Patent 5,683,866